Author Manuscript

Author Manuscript

Author Manuscript

Author Manuscript

HHS Public Access

Author manuscript

Nano Lett. Author manuscript; available in PMC 2018 March 28.

Published in final edited form as:

Nano Lett. 2016 October 12; 16(10): 6265–6271. doi:10.1021/acs.nanolett.6b02557.

A Nanoscale Tool for Photoacoustic-Based Measurements of Clotting Time and Therapeutic Drug Monitoring of Heparin

Junxin Wang[†], **Fang Chen**[†,‡], **Santiago J. Arconada-Alvarez**[†], **James Hartanto**[†], **Li-Peng Yap**[§], **Ryan Park**[§], **Fang Wang**[†,‖], **Ivetta Vorobyova**[§], **Grant Dagliyan**[§], **Peter S. Conti**[§], and **Jesse V. Jokerst**[†,‡,*]

[†]Department of NanoEngineering, University of California San Diego, La Jolla, California 92093, United States

[‡]Materials Science and Engineering Program, University of California San Diego, La Jolla, California 92093, United States

[§]Molecular Imaging Center, University of Southern California Keck School of Medicine, Los Angeles, California 90089, United States

[‖]University of Science and Technology Beijing, Research Center for Bioengineering and Sensing Technology, Beijing 100083, People's Republic of China

Abstract

Heparin anticoagulation therapy is an indispensable feature of clinical care yet has a narrow therapeutic window and is the second most common intensive care unit (ICU) medication error. The active partial thromboplastin time (aPTT) monitors heparin but suffers from long turnaround times, a variable reference range, limited utility with low molecular weight heparin, and poor correlation to dose. Here, we describe a photoacoustic imaging technique to monitor heparin concentration using methylene blue as a simple and Federal Drug Administration-approved contrast agent. We found a strong correlation between heparin concentration and photoacoustic signal measured in phosphate buffered saline (PBS) and blood. Clinically relevant heparin concentrations were detected in blood in 32 s with a detection limit of 0.28 U/mL. We validated this imaging approach by correlation to the aPTT (Pearson's $r = 0.86$; $p < 0.05$) as well as with protamine sulfate treatment. This technique also has good utility with low molecular weight heparin (enoxaparin) including a blood detection limit of 72 μg/mL. We then used these findings to create a nanoparticle-based hybrid material that can immobilize methylene blue for potential

*Corresponding Author: jjokerst@ucsd.edu.

Author Contributions

J.W. and J.V.J. designed and performed the experiments and wrote the paper. F.C. assisted the fabrication of nanoparticle and conceived the strategy of its surface modification. S.J.A., J.H., and F.W. helped perform the experiments. L.Y., R.P., I.V., G.D., and P.S.C. provided facilities for photoacoustic imaging.

Notes

The authors declare no competing financial interest.

Supporting Information

The Supporting Information is available free of charge on the ACS Publications website at DOI: 10.1021/acs.nano-lett.6b02557.
(I) Stability and reproducibility of methylene blue/heparin complex; (II) mechanism of the binding between methylene and heparin; (III) utility of photoacoustic imaging in whole blood (PDF)
Real-time reversibility test in blood (AVI)

Author Manuscript Author Manuscript Author Manuscript Author Manuscript

applications as a wearable/implantable heparin sensor to maintain drug levels in the therapeutic window. To the best of our knowledge, this is the first use of photoacoustics to image anticoagulation therapy with significant potential implications to the cardiovascular and surgical community.

Graphical Abstract

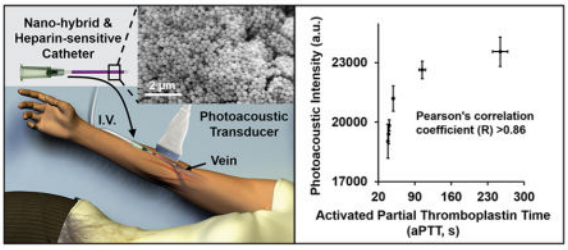

Keywords

Anticoagulation therapy; silica nanoparticles; therapeutic drug monitoring; photoacoustic imaging; optoacoustics; heparin; partial thromboplastin time

Heparin anticoagulation therapy is a cornerstone of surgical and cardiovascular medicine because of its short half-life, easy reversibility, and low cost.[1–3] It is used prophylactically in angiography (2 million cases/year),[4] coronary bypass (0.5 million cases/year),[5] cannulation, [6] and extracorporeal membrane oxygenation[7] as well as therapeutically for thromboses (300 thousand/year)[8] with over 500 million doses given annually worldwide.[9] This highly sulfated and negatively charged glycosaminoglycan increases the activity of antithrombin 1000-fold to inactivate the clotting factors thrombin and Factor Xa.[10]

However, heparin anticoagulation therapy is challenged by its variable molecular weight, activity, and biodistribution.[1] Heparin has a narrow therapeutic window and is the second most common ICU medication error.[11] These inherent challenges are compounded by iatrogenic errors such as incorrect heparin dosage, inaccurate infusion pump settings, and incomplete recordkeeping resulting in ~10 000 heparin medication errors per year.[12] Heparin therapy is especially challenging in pediatric patients because of their rapidly changing hemostasis system, guidelines based on adults, and challenges in collecting sufficient blood volumes.[3,13] This results in thousands of children with hemorrhages or emboli annually.[14]

Because of these issues, heparin therapy must be carefully monitored with the activated partial thromboplastin time (aPTT) per nomogram and serves as a surrogate test for inactivation of numerous clotting factors including XIIa, Xia, and IXa.[15] However, this in vitro diagnostic blood test suffers from long turnaround times, a variable reference range, limited utility with low molecular weight heparin (LMWH), and broad intra- and interassay variance. More importantly, the aPTT is only a surrogate for heparin activity because it measures the conversion of fibrinogen to fibrin rather than antithrombin activity.[16] While anti-Xa analysis offers a more sophisticated metric of anticoagulation,[17] this test still has a

Author Manuscript Author Manuscript Author Manuscript Author Manuscript

long turnaround time and is limited to large research hospitals. Thromboelastography or the activated clotting time are established in the operating room, but are operator intensive, invasive, and time-consuming.[18] Furthermore, all of these tools are limited by the low frequency with which blood can be sampled. While point-of-care testing can improve the frequency with which the aPTT is measured,[19] it still requires an operator to collect and prepare blood samples and is inaccurate at higher concentrations.[20] Thus, real-time and noninvasive tools to monitor heparin anticoagulation therapy could markedly improve the standard of care; one such approach to solving these limitations is imaging rather than in vitro diagnostics.

Tools to image anticoagulation must have good sensitivity, contrast, and temporal resolution —photoacoustic imaging is a novel technique that has these features. It uses a nanosecond laser pulse to generate thermal expansion and a pressure change for acoustic detection. It combines the high contrast of optical imaging with the speed of ultrasound. Photoacoustic imaging can use endogenous contrast such as hemoglobin and melanin[21–23] as well as exogenous contrast[24,25] including small molecules like methylene blue[26,27] and nanoparticles.[28–32] While photoacoustic flow cytometry has measured emboli based on the absorption change and nanosensors have been reported for therapeutic drug monitoring of lithium,[33] there is no approach to monitoring heparin therapy with acoustics.[34,35]

Here, we describe a simple tool to quickly measure the concentration of heparin in both buffer and whole human blood using photoacoustic imaging. This work is inspired by colorimetric or optical methods[36–40] that measure heparin through a spectral shift or intensity change but that failed when used in whole blood. In contrast, we found that the photoacoustic signal of the clinically approved methylene blue dye increases dramatically upon binding to heparin (see Materials and Methods in Supporting Information). Methylene blue (Figure 1a) is already used to visualize sentinel lymph nodes[41] and has broad absorption peaks between 500 and 700 nm (Figure 1b) but only nominal photoacoustic signal in the optical window typically used for imaging (680–900 nm; sensitivity of 7.1 μM at 680 nm, Figure S1a,d). When electrostatically coupled to heparin (Figure 1c), however, the absorption (Figure 1b) and color of methylene blue changes (inset Figure 1b). Somewhat surprisingly, this heparin complexation also produces an intense (Figure 1d) increase in photoacoustic signal.

We optimized the methylene blue concentration as a function of signal upon 6.4 U/mL heparin addition and found that 0.6 mM methylene blue produced the best contrast when added to heparin versus free methylene blue only in buffer (Figure S1b,e); this was used for all subsequent buffer-based experiments. Linear regression shows a strong correlation between photoacoustic signal and heparin concentration from 0 to 6.4 U/mL (exponential linear regression $R^2 > 0.98$) with a detection limit of 14.2 mU/mL (Figure 1e). Spectral photoacoustic imaging of these samples showed a maximal intensity absorbance at 680 nm with a characteristic peak near 710 nm (arrow in Figure 1f) and a 30-fold increase in photoacoustic signal with 6.4 U/mL heparin at 710 nm excitation. Heparin concentrations over 10 U/mL show decreased signal. Although further studies are needed to understand the mechanism underlying this decrease, possible reasons include aggregation of heparin or a phenomenon analogous to the “hook effect” seen in ELISA.[42] The relative standard

Author Manuscript Author Manuscript Author Manuscript Author Manuscript

deviation (RSD) of interassay (Figure S1c) variation is <12%, and the signal is temporally stable (RSD < 15%; Figure S1f).

This signal was reversible via the known heparin antagonist protamine sulfate. Protamine reverses heparin overdose or deheparinizes patients after surgery at a ratio of 10 μg per 1 U heparin.[43] We found that the photoacoustic signal of the 5 U samples was completely neutralized with 50 μg of protamine sulfate and this is in agreement with the reported dosing guidelines (Figure 2a); the absorbance spectra returned to baseline after protamine sulfate treatment (Figure 1b). The spectral fingerprint at 710 nm also disappears upon addition of protamine sulfate (Figure 1f). Photoacoustic signal linearly decreases as a function of protamine sulfate concentration ($R^2 > 0.94$; Figure 2b). As an initial test to validate the clinical compatibility of this assay, we studied the effect of antithrombin. There was no change in the photoacoustic signal when 40 μg of human antithrombin III was added to heparin and methylene blue (Figure S2a).

Similar data were collected with LMWH (Figure 2c,d). The photoacoustic intensity of methylene blue treated with 1.6 mg/mL LMWH (enoxaparin sodium) is 7-fold higher than the signal of methylene blue only with a detection limit of 1.4 μg/mL. The photoacoustic spectrum of LMWH also showed a peak at around 710 nm at concentrations over 5 U/mL (arrow in Figure 1f). This spectral feature could potentially discriminate the heparin- or LMWH-specific signal from the photoacoustic signal of hemoglobin, deoxyhemoglobin, or melanin.

The photoacoustic signal is generated by methylene blue/heparin complex. Methylene blue has a net positive charge via the sulfonium and nitrogen groups that can associate with heparin's negative charge. This causes a partial charge transfer to decrease the π-electron energy on the dye and increase the transition energy to $\Delta E = 2.304$ eV or a λ_{max} of ~ 550 nm.[44] The absorption from 719–850 nm increases 1–35% with 6.4 U/mL heparin (Figure S2b). To measure any background signal from the heparin/protamine complex, we measured these species in a phantom. While an increased absorbance (due to scatter) was noted, no photoacoustic signal was seen (Figure S2c,d) because there is no chromophore.

It seems unlikely that either the small increase in near IR absorbance or fluorescence quenching (Figure S2e) is responsible for the large increase in photoacoustic signal. The heparin binding likely causes methylene blue to have faster heat transfer to the solvent. When the small molecule is more strongly associated with the heparin polymer than the solvent, more of its absorbed incident energy is released as photo-acoustic thermal expansion than vibrational energy to water molecules. This is analogous to the reduced interfacial thermal resistance seen with silica-coated gold nanorods.[45] The signal reversibility via protamine helps confirm this hypothesis. Protamine has a higher positive charge than methylene blue, and it has greater affinity for heparin. This photoacoustic signal decreases as methylene blue becomes dissociated from heparin due to heparin/protamine binding.

We next validated this technique in blood. Blood contains hemoglobin and deoxyhemoglobin that can also produce photoacoustic signal[21] and thus validating this

Author Manuscript Author Manuscript Author Manuscript Author Manuscript

approach in blood was an important next step. We used a slightly higher concentration of methylene blue in the blood experiments (0.8 mM) because the hemoglobin in whole blood can increase photoacoustic baseline signal. While there was a signal increase when methylene blue was added to blood (Figure S3a), the addition of heparin increased this signal even further. Blood samples ($n = 3$) with 0.025, 0.05, 0.1, 0.2, and 0.4 U/mL heparin and 0.8 mM methylene blue provides 2, 4, 11, 19, and 24% higher signal than blood with 0.8 mM methylene blue only, respectively (Figure 3a,b). The RSDs of these samples were <8% with a logarithmic regression of $R^2 > 0.97$. The detection limit was 0.28 U/mL, and the signal was stable (<5% variation) for at least 15 min (Figure S3b). This is much more stable than the value seen in buffer (Figure S1f); the lower signal stability in buffer may be due to more association/dissociation events due to fewer stabilizing proteins.

We also studied blood with higher heparin concentrations, and blood/methylene with 5 U/mL had 20-fold higher signal than blood with 0 U/mL heparin (Figure S3c). Importantly, the decreased signal intensity seen at high concentrations in buffer was not present in blood perhaps because the albumin and other serum proteins stabilize the methylene blue/heparin complex.

Although the aPTT has shown variable correlation to heparin dose in human trials,[46] we next used aPTT testing to confirm the clinical relevance of this assay; samples were studied with both the imaging technique and the aPTT. The aPTT values were typical of human therapy (30–300 s). When these values were plotted versus the aPTT (Figure 3c), regression analysis showed good correlation between clotting time and photo-acoustic signal (Pearson's $r = 0.86$; $p < 0.05$) suggesting that this imaging data is representative of actual clotting time.

To study the temporal features of photoacoustics, we measured the time between heparin or protamine injection and signal increase in a methylene blue/human blood sample placed in a customized flow chamber. The photoacoustic signal increased 3.6-fold 31 s after the injection of 0.1 mL of 50 U/mL heparin (working concentration of 3 U/mL) in to 1.7 mL of blood/methylene blue complex (methylene blue concentration of 0.8 mM) (Figure 3d; Video S1). It took 32 s for the signal to decrease back to baseline after injection of 0.1 mL of 0.5 mg/mL protamine (Figure 3d). The delay between drug injection and photoacoustic signal enhancement or reduction could be due to the slow drug diffusion in the blood. Nevertheless, photoacoustics shows strong advantage in time compared to the current gold standard method (aPTT). We note that the signal increase here is lower than observed in Figure S3c. This is because the 2 mm thick plastic walls of the custom flow chamber.

Protamine sulfate reversal was further quantified in blood samples. The signal was significantly ($p < 0.01$) reduced when 80 μg of protamine was added to the heparinized blood (Figure 3e). Spectral data (Figure S3d) confirmed the reversal of methylene blue/heparin binding, although the spectra of the methylene blue/heparin complex was slightly different from the spectra measured in buffer (Figure 1f) due to the presence of erythrocytes. The characteristic peak at 710 nm only occurred at more than 50 U/mL heparin in blood. This could potentially be used to signal an overdose event.

Author Manuscript Author Manuscript Author Manuscript Author Manuscript

We noted similar signal enhancements with LMWH (Figure 3f) and the imaging signal correlates to LMWH concentration ($R^2 > 0.97$; Figure 3f). The signal enhancement with 160 μg/mL LMWH and 0.8 mM methylene blue is 35% higher than methylene blue only with a limit of detection of 72 μg/mL. This is important because LMWH is currently monitored with the anti-Factor Xa ELISA testing;[47] the aPTT cannot monitor LMWH therapy.[47,48] Thus, future work will be dedicating to improving the LMWH utility.

The correlation between the photoacoustic data and the aPTT, as well as the protamine sulfate-based deheparinization, confirms that the imaging signal offers functional information about blood clotting time. This approach is sensitive to clinically relevant heparin concentrations. We showed a sensitivity of 14.2 mU/mL in buffer and 0.28 U/mL in whole blood. These detection limits are lower than the concentrations used in thromboembolism (7–8 U/mL, 35 000–40 000 U/24 h),[49] acute myocardial infarction (2.5 U/mL,12 500 U/12 h),[50] coronary angioplasty (2 U/mL),[51] and cardiopulmonary bypass (5.6 U/mL)[52] as well as the lower doses used in treatment of extracorporeal membrane oxygenation 0.5 U/mL (50 U/kg).[53] These concentrations all assumed a blood pool volume of 5 L.

Methylene blue is already FDA-approved with minimal effects on anticoagulation.[54] This approach could be developed for fingerprick samples and a bedside photoacoustic analyzer. However, to better harness the capabilities of imaging we envision a wearable, heparin-sensitive catheter that not only delivers heparin but also monitors clotting time. To encapsulate the dye on a usable substrate, we created a hybrid of agar gel and silica nanoparticles that could be coated on the surface of the catheter. Simply mixing methylene blue with agarose resulted in quick release of 40% of the dye (Figure 4a). While methylene blue could be stably bound to Stober silica nanoparticles (SSNP in Figure 4b,c), there was no photo-acoustic response when heparin was added. The surface charge of these nanoparticle is −23 mV, which is too negative to allow association between the nanoparticle-bound dye and negatively charged heparin. Therefore, careful nanoengineering was required to produce a material that was both stable and responsive to heparin.

To tune the nanoparticles, we treated them with (3-mercaptopropyl)trimethoxysilane (MPTMS) to adjust the zeta potential to −15 mV (SSNP-SH in Figure 4b,c). We used this material with agar gel to create a coating on a catheter tube (Figure 5a). Absorption data showed that the hybrid material has a methylene blue concentration of 1.5 mM with low methylene blue release (<10%) after 40 min incubation in PBS (Figure 4a). More importantly, the methylene blue on these modified nanoparticles remain responsive to heparin with 51% more photoacoustic signal at 10 U/mL heparin than PBS (Figure 5b) for 1 h incubation. The signal enhancement was stable after constant imaging at 680 nm for 9 min (RSD < 4%) (Figure 4d). This system was also reversible. When the 50 U/ mL-treated device was reversed with protamine (8 mg/mL), the signal decreased by 42% versus no protamine treatment (Figure 5b). The higher signal of the heparin-treated hybrid versus PBS-treated hybrid is likely due to interactions between methylene blue and heparin, which increases the photoacoustic signal and decreases diffusion of this complex and free methylene blue into solution.

Author Manuscript Author Manuscript Author Manuscript Author Manuscript

The strengths of this approach include the rapid turnaround time, excellent sensitivity, good correlation to the aPTT, and flexibility with both heparin and LMWH. While the aPTT is the gold standard for monitoring anticoagulation, it suffers from long turnaround times and limited utility with LMWH. In contrast, it only takes 0.2 s for photoacoustic imaging to acquire one data point (5 Hz imaging) and can be used with both unfractionated and LMWH, although more than one frame might be needed for accurate and stable signal. This approach could also leverage spectral or ratiometric imaging to decouple the heparin-specific signal from other sources of photoacoustic signal.

Limitations to this approach include different PA background due to hydration state, oxygenation, body fat content, and location of the catheter. However, we will monitor the change in signal versus baseline as a function of heparin therapy to control for these variations. This approach also does not discriminate between the anticoagulant and nonanticoagulant glycosaminoglycan sequences on heparin or LMWH; these are similar to all other existing tools to monitor heparin. In addition, the current generation of the nanoparticle hybrid has a slower response (~1 h) than free methylene blue in blood (~30 s) because of the porous nature of the agar/nanoparticle hybrid material and the longer time needed for the heparin to diffuse into the gel network as well as the time kinetics of methylene blue release from the nanoparticle to associate with the heparin. Future work is refining this device for faster responses.

Most importantly, we do show that the photoacoustic signal correlates to activity and this is the key metric of interest to clinicians. We also show no activation by endogenous glycosaminoglycans (Figure S3a). Although there are a wide variety of species present in blood, we can still detect clinically relevant heparin concentrations above this background (Figure S3a).

Future work will include the use of photoacoustic signal processing and other phenothiazinium derivatives to increase the sensitivity and specificity. Blood processing, phlebotomy protocols, surgery type,[55] and donor health can all affect the signal contrast between the probe and probe/heparin and will be optimized. Ongoing work will continue to refine this hybrid catheter for use with animal models of anticoagulation therapy. When implanted, this would allow heparin therapy to be monitored without a blood sample.

In this paper, we report for the first time that methylene blue has a significant and dose-dependent increase in photoacoustic signal in the presence of both heparin and LMWH. This signal was validated in both buffer and whole blood with good correlation to the gold standard aPTT; the signal was reversible with protamine sulfate deheparinization. Photoacoustic imaging is a real time technique, and methylene blue is a FDA-approved dye. Thus, this method is promising for real-time monitoring of anticoagulation therapy to quickly titrate the patient into the therapeutic window. This has potentially profound implications because acoustics-based wearable sensors would have low costs, good transmission through tissue without scatter/diffusion, no ionizing radiation, and high temporal and spatial resolution in contrast to many optical or electrical sensors.

Author Manuscript Author Manuscript Author Manuscript Author Manuscript

Supplementary Material

Refer to Web version on PubMed Central for supplementary material.

Acknowledgments

J.V.J. acknowledges funding from NIH HL117048 HL137187 and infrastructure from S10 OD021821; P.S.C. acknowledges S10 RR02365. We thank Dr. Dzung Le and Qiongyu Chen for their help in the aPTT measurements. We also thank Lu Yang for the assistance in taking SEM images.

References

1. Hirsh J, Anand SS, Halperin JL, Fuster V. American Heart, A. Circulation. 2001; 103(24):2994–3018. [PubMed: 11413093]
2. Monagle P, Chan AK, Goldenberg NA, Ichord RN, Journeycake JM, Nowak-Gottl U, Vesely SK. American College of Chest, P. Chest. 2012; 141(2):e737S–e801S. [PubMed: 22315277]
3. Newall F, Johnston L, Ignjatovic V, Monagle P. Pediatrics. 2009; 123(3):e510–8. [PubMed: 19221154]
4. Cook S, Walker A, Hügli O, Togni M, Meier B. Clin Res Cardiol. 2007; 96(6):375–382. [PubMed: 17453137]
5. Ţintoiu, IC, Underwood, MJ, Cook, SP, Kitabata, H, Abbas, A. Coronary Graft Failure: State of the Art. Springer; New York: 2016.
6. Pasquali SK, Li JS, Burstein DS, Sheng S, O'Brien SM, Jacobs ML, Jaquiss RD, Peterson ED, Gaynor JW, Jacobs JP. Pediatrics. 2012; 129(2):e370–6. [PubMed: 22232310]
7. Maslach-Hubbard A, Bratton SL. World journal of critical care medicine. 2013; 2(4):29–39. [PubMed: 24701414]
8. Goldenberg, NA, Manco-Johnson, MJ. Pediatric thrombotic disorders. Cambridge University Press; New York: 2015.
9. Buchanan, MR, Ofosu, FA, Brister, SJ. ThrombinIts Key Role in Thrombogenesis-Implications for Its Inhibition. CRC Press; Boca Raton, FL: 1994.
10. Rosenberg RD. Federation proceedings. 1985; 44(2):404–9. [PubMed: 3155697]
11. Wahr JA, Shore AD, Harris LH, Rogers P, Panesar S, Matthew L, Pronovost PJ, Cleary K, Pham JC. American journal of medical quality: the official journal of the American College of Medical Quality. 2014; 29(1):61–9. [PubMed: 23656705]
12. Grissinger MC, Hicks RW, Keroack MA, Marella WM, Vaida AJ. Joint Commission journal on quality and patient safety/Joint Commission Resources. 2010; 36(5):195–202.
13. Kaushal R, Bates DW, Landrigan C, McKenna KJ, Clapp MD, Federico F, Goldmann DA. Jama. 2001; 285(16):2114–20. [PubMed: 11311101]
14. Arimura J, Poole RL, Jeng M, Rhine W, Sharek P. journal of pediatric pharmacology and therapeutics: JPPT: the official journal of PPAG. 2008; 13(2):96–8.
15. Raschke RA, Reilly BM, Guidry JR, Fontana JR, Srinivas S. Ann Intern Med. 1993; 119(9):874–81. [PubMed: 8214998]
16. Key, N, Makris, M, O'Shaughnessy, D, Lillicrap, D. Practical hemostasis and thrombosis. Wiley Online Library; Hoboken, NJ: 2009.
17. Liveris A, Bello RA, Friedmann P, Duffy MA, Manwani D, Killinger JS, Rodriquez D, Weinstein S. Pediatric Critical Care Medicine. 2014; 15(2):e72–e79. [PubMed: 24335992]
18. Lang T, von Depka M. Hämostaseologie. 2006; 26(5):20–29.
19. Nichols JH, Christenson RH, Clarke W, Gronowski A, Hammett-Stabler CA, Jacobs E, Kazmierczak S, Lewandrowski K, Price C, Sacks DB. Clin Chim Acta. 2007; 379(1–2):14–28. [PubMed: 17270169]
20. Gertler R, Wiesner G, Tassani-Prell P, Braun SL, Martin K. J Cardiothorac Vasc Anesth. 2011; 25(6):981–986. [PubMed: 21315618]

Author Manuscript Author Manuscript Author Manuscript Author Manuscript

21. Zhang HF, Maslov K, Sivaramakrishnan M, Stoica G, Wang LHV. Appl Phys Lett. 2007; 90(5): 053901.
22. Wang LV, Hu S. Science. 2012; 335(6075):1458–62. [PubMed: 22442475]
23. Zhang HF, Maslov K, Stoica G, Wang LV. Nat Biotechnol. 2006; 24(7):848–51. [PubMed: 16823374]
24. Luke GP, Yeager D, Emelianov SY. Ann Biomed Eng. 2012; 40(2):422–37. [PubMed: 22048668]
25. Huynh E, Lovell JF, Helfield BL, Jeon M, Kim C, Goertz DE, Wilson BC, Zheng G. J Am Chem Soc. 2012; 134(40):16464–16467. [PubMed: 22827774]
26. Song KH, Stein EW, Margenthaler JA, Wang LV. J Biomed Opt. 2008; 13(5):054033. [PubMed: 19021413]
27. Erpelding TN, Kim C, Pramanik M, Jankovic L, Maslov K, Guo Z, Margenthaler JA, Pashley MD, Wang LV. Radiology. 2010; 256(1):102–110. [PubMed: 20574088]
28. Galanzha EI, Shashkov EV, Kelly T, Kim JW, Yang L, Zharov VP. Nat Nanotechnol. 2009; 4(12): 855–860. [PubMed: 19915570]
29. Lovell JF, Jin CS, Huynh E, Jin H, Kim C, Rubinstein JL, Chan WCW, Cao W, Wang LV, Zheng G. Nat Mater. 2011; 10(4):324–332. [PubMed: 21423187]
30. Zerda, Adl; Liu, Z; Bodapati, S; Teed, R; Vaithilingam, S; Khuri-Yakub, BT; Chen, X; Dai, H; Gambhir, SS. Nano Lett. 2010; 10(6):2168–2172. [PubMed: 20499887]
31. Pu K, Shuhendler AJ, Jokerst JV, Mei J, Gambhir SS, Bao Z, Rao J. Nat Nanotechnol. 2014; 9(3): 233–239. [PubMed: 24463363]
32. Weber J, Beard PC, Bohndiek SE. Nat Methods. 2016; 13(8):639–650. [PubMed: 27467727]
33. Cash KJ, Li C, Xia J, Wang LV, Clark HA. ACS Nano. 2015; 9(2):1692–1698. [PubMed: 25588028]
34. Galanzha EI, Zharov VP. Methods. 2012; 57(3):280–96. [PubMed: 22749928]
35. Juratli MA, Menyaev YA, Sarimollaoglu M, Siegel ER, Nedosekin DA, Suen JY, Melerzanov AV, Juratli TA, Galanzha EI, Zharov VP. PLoS One. 2016; 11(5):e0156269. [PubMed: 27227413]
36. Zhong Z, Anslyn EV. J Am Chem Soc. 2002; 124(31):9014–9015. [PubMed: 12148981]
37. Cao R, Li B. Chem Commun. 2011; 47(10):2865–7.
38. Fu X, Chen L, Li J, Lin M, You H, Wang W. Biosens Bioelectron. 2012; 34(1):227–31. [PubMed: 22387039]
39. Cai L, Zhan R, Pu KY, Qi X, Zhang H, Huang W, Liu B. Anal Chem. 2011; 83(20):7849–7855. [PubMed: 21882808]
40. Fu X, Chen L, Li J. Analyst. 2012; 137(16):3653–3658. [PubMed: 22741162]
41. Simmons R, Thevarajah S, Brennan MB, Christos P, Osborne M. Annals of Surgical Oncology. 2003; 10(3):242–247. [PubMed: 12679308]
42. Butch AW. Clinical Chemistry. 2000; 46(10):1719–1720. [PubMed: 11017960]
43. Lowary LR, Smith FA, Coyne E, Dunham NW. J Pharm Sci. 1971; 60(4):638–640. [PubMed: 5128383]
44. Luo HQ, Liu SP, Liu ZF, Liu Q, Li NB. Anal Chim Acta. 2001; 449(1–2):261–270.
45. Chen YS, Frey W, Kim S, Kruizinga P, Homan K, Emelianov S. Nano Lett. 2011; 11(2):348–354. [PubMed: 21244082]
46. Kuhle S, Eulmesekian P, Kavanagh B, Massicotte P, Vegh P, Lau A, Mitchell LG. Haematologica. 2007; 92(4):554–557. [PubMed: 17488668]
47. Boneu, B, de Moerloose, P. How and when to monitor a patient treated with low molecular weight heparin. Thieme Medical Publishers, Inc; New York: 2001. 519–522. Seminars in thrombosis and hemostasis
48. Barrowcliffe TW. Br J Haematol. 1995; 90(1):1–7. [PubMed: 7786769]
49. Gould MK, Dembitzer AD, Doyle RL, Hastie TJ, Garber AM. Ann Intern Med. 1999; 130(10): 800–9. [PubMed: 10366369]
50. The Scati (Studio Sulla Calciparina Nell'Angina E Nella Trombosi Ventricolare Nell'Infarto) Group. Lancet. 1989; 334(8656):182–186. DOI: 10.1016/S0140-6736(89)90371-1

Author Manuscript Author Manuscript Author Manuscript Author Manuscript

51. Narins CR, Hillegass WB, Nelson CL, Tcheng JE, Harrington RA, Phillips HR, Stack RS, Califf RM. Circulation. 1996; 93(4):667–671. [PubMed: 8640994]
52. Wright SJ, Murray WB, Hampton WA, Hargovan H. J Cardiothorac Vasc Anesth. 1993; 7(4):416–421. [PubMed: 8400096]
53. Baird CW, Zurakowski D, Robinson B, Gandhi S, Burdis-Koch L, Tamblyn J, Munoz R, Fortich K, Pigula FA. Annals of thoracic surgery. 2007; 83(3):912–920. [PubMed: 17307433]
54. Kikura M, Lee MK, Levy JH. Anesth Analg. 1996; 83(2):223–227. [PubMed: 8694296]
55. Seyfer AE, Seaber AV, Dombrose FA, Urbaniak JR. Ann Surg. 1981; 193(2):210–213. [PubMed: 7469554]

Author Manuscript Author Manuscript Author Manuscript Author Manuscript

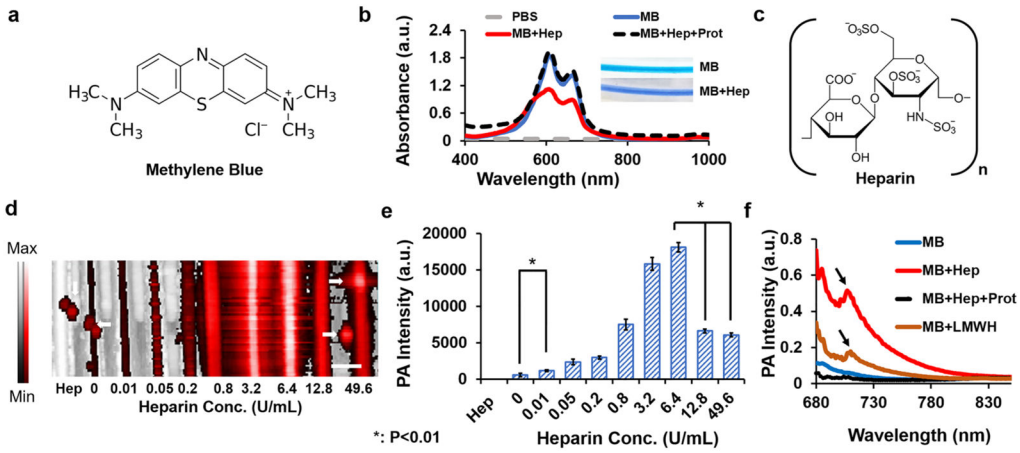

Figure 1.

Photoacoustic changes to methylene blue in the presence of heparin. (a) Chemical structure of methylene blue showing delocalized positive charge. (b) In the presence of 6.4 U/mL heparin, 0.6 mM methylene blue has a decrease in absorbance between 573 to 718 nm and a slight increase over 719 nm (see Figure S2b); these changes reverse upon addition of 8 mg/mL protamine. Inset in panel b represents the color change in methylene blue (MB) upon binding to heparin (MB+Hep). (c) Chemical structure of heparin with negative charge. Panel d shows imaging data of a phantom using 0.6 mM methylene blue and increasing concentrations of heparin. The image is a maximum intensity projection of photoacoustic data overlaid on ultrasound (B-mode) data. The black-to-white bar corresponds to ultrasound intensity, and the black-to-red bar corresponds to photoacoustic data. We noted a linear response between 0 and 6.4 U/mL of heparin. White arrows indicate dust particles producing extraneous signal. (e) Statistical analysis quantifies the data in (d) including a detection limit of 14.2 mU/mL and exponential linear regression ($R^2 > 0.98$) from 0 to 6.4 U/mL. (f) Photoacoustic spectral data of the 6.4 U/mL sample shows a peak near 710 nm that is characteristic of the heparin and LMWH binding (arrows). This peak and the overall magnitude of the photoacoustic signal change decreases with protamine sulfate addition. Here, PA, MB, Hep, and Prot stand for photoacoustic, methylene blue, heparin, and protamine, respectively. The scale bar in (d) is 3 mm.

Author Manuscript Author Manuscript Author Manuscript Author Manuscript

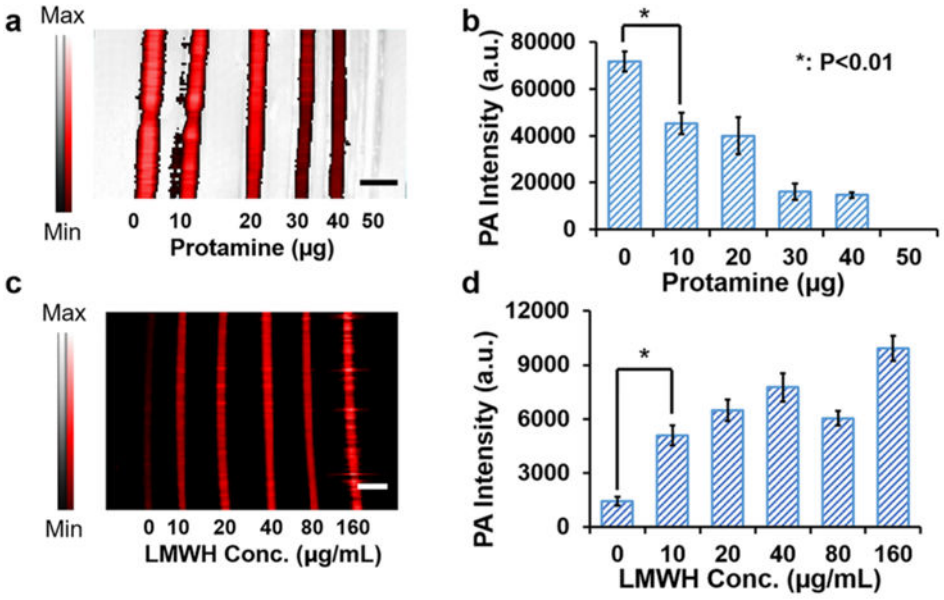

Figure 2.

Signal reversibility and use with LMWH. (a,b) Protamine sulfate caused a dose-dependent decrease in photoacoustic signal when added to a 5 U heparin solution. This relationship was linear at $R^2 > 0.94$, and complete neutralization occurred at 50 μg of protamine sulfate (known stoichiometry is 10 μg per 1 U heparin[43]). (c,d) Photoacoustic imaging can also be used to monitor LMWH with a detection limit of 1.4 μg/mL. Scale bars in (a,c) are 3 mm. Error bars represent the standard deviation.

Author Manuscript Author Manuscript Author Manuscript Author Manuscript

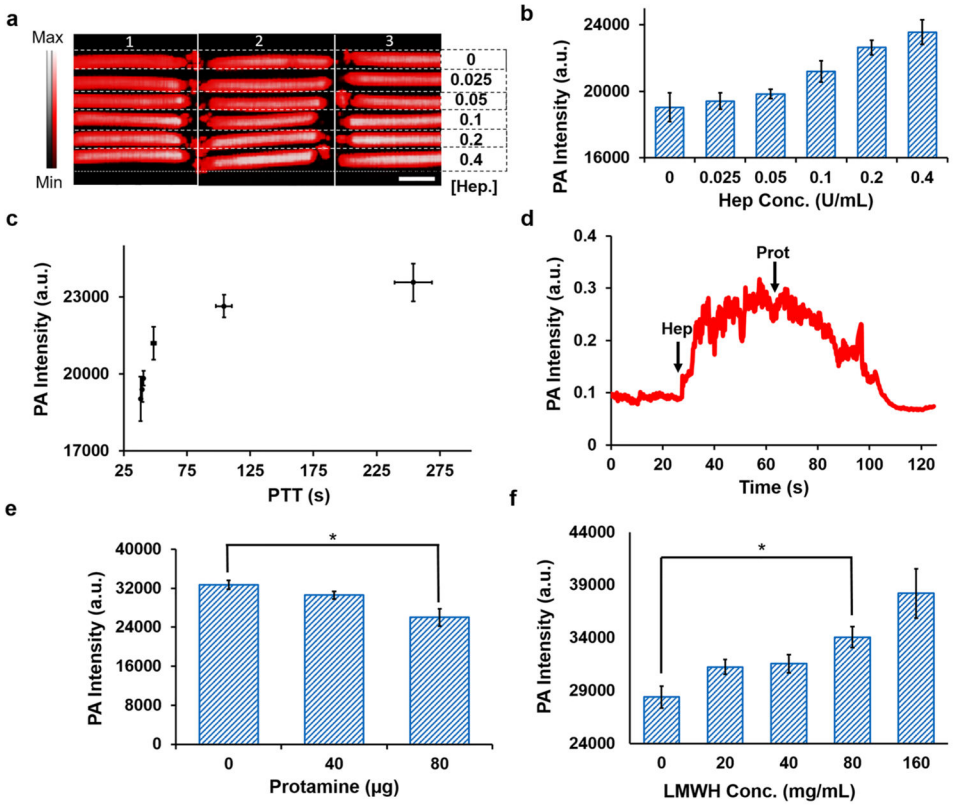

Figure 3.

Photoacoustic signal in whole human blood. (a) Photoacoustic image of plastic tubing containing human blood with 0.8 mM methylene blue and increasing concentrations of heparin with 0.8 mM methylene blue ($n = 3$ replicates). Scale bar in (a) is 3 mm. Panel b quantitates the three replicates in panel a, and the detection limit of heparin is 0.28 U/mL. Panel c plots the photoacoustic intensity versus aPTT. The Pearson's correlation coefficient (r) was 0.86; $p < 0.05$). Panel d shows the photoacoustic signal changes of blood/methylene blue mixture as a function of time when heparin (at 27 s) and protamine (at 68 s) were added. Panel e shows that the heparin signal is reversible in whole blood with titration of protamine—the known heparin antagonist. (f) This approach also has utility with increasing concentrations of LMWH in methylene blue-doped human blood; the lowest concentration of LMWH can be detected in blood is 72 μg/mL. Error bars represent the standard error. *: $p < 0.01$.

Author Manuscript Author Manuscript Author Manuscript Author Manuscript

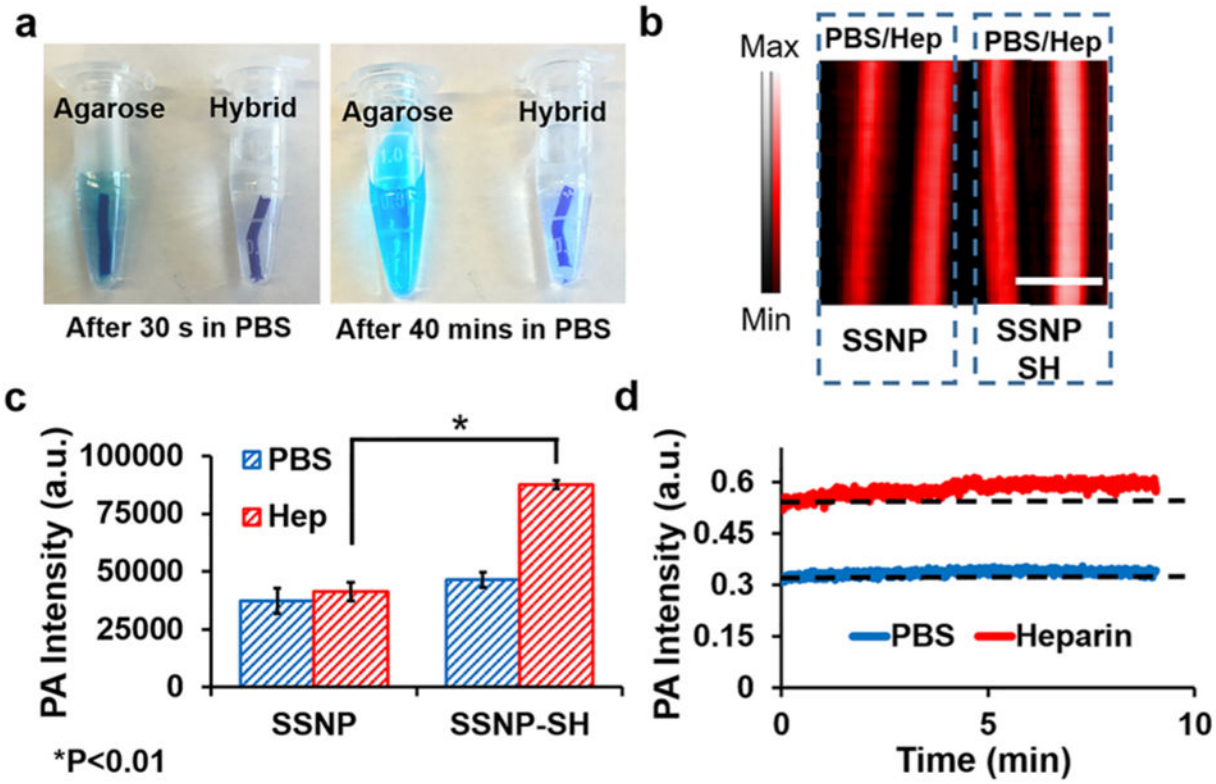

Figure 4.

Optimization of material for a heparin-responsive catheter. (a) Methylene blue in agarose was not stable with more than 40% methylene blue release in PBS after 40 min. The addition of nanoparticles for a hybrid material reduced this release to less than 10%. (b) Photoacoustic images of methylene blue loaded on as-made silica nanoparticles (SSNP; −23 mV) and methylene blue loaded on thiol-coated silica nanoparticles (SSNP-SH; −15 mV). Both were treated with PBS and heparin (Hep) but only the thiol-coated nanoparticles were responsive to heparin. The lower ζ-potential facilitated the photoacoustic signal increase. (c) Methylene blue-loaded SSNP-SH treated with heparin offers significantly more signal than SSNP-SH treated with PBS or SSNP. (d) The nanoparticle/agar hybrid material was treated with PBS or 10 U/mL heparin and imaged at 680 nm for 9 min with no decrease in signal.

Author Manuscript Author Manuscript Author Manuscript Author Manuscript

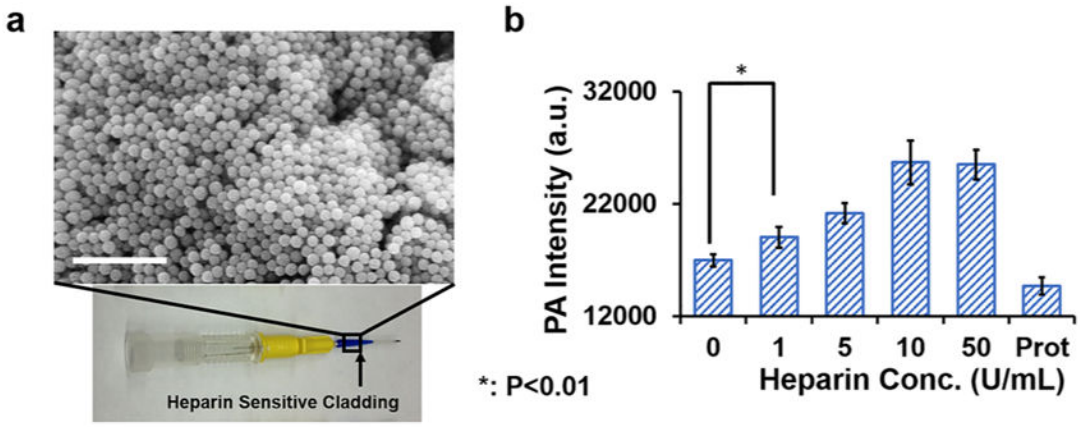

Figure 5.

Sensitivity of the hybrid material in detecting heparin. (a) The proposed device uses methylene-blue coated nanoparticles embedded in agar and coated on the exterior of a venous catheter. This would be used for in vivo anticoagulation monitoring. The inset is a scanning electron microscope image of the agarose/silica nano-particle hybrid. (b) This design was used to measure increasing concentrations of heparin as well as a protamine control. Scale bar in panel a is 2 μm.